

Compact Silicon Photonic Interleaver Using an Interfering Loop Containing a Fabry-Perot Cavity Formed by Sagnac Loop Mirrors

Xinhong Jiang, Yuxing Yang, Boyu Liu, Yong Zhang, Ciyuan Qiu, and Yikai Su

State Key Lab of Advanced Optical Communication Systems and Networks, Department of Electronic Engineering, Shanghai Jiao Tong University, Shanghai 200240, China, yikaisu@sjtu.edu.cn

Abstract: A compact ($106.4 \times 55.1 \mu\text{m}^2$) silicon photonic interleaver is proposed and experimentally demonstrated. The 3-dB and 20-dB bandwidths of the passband are $\sim 1.09 \text{ nm}$ and $\sim 1.585 \text{ nm}$, respectively. The central wavelength can be changed by tuning only one waveguide.

Introduction

In a wavelength division multiplexed (WDM) system, an interleaver can be used to combine or divide odd and even channels to suppress neighboring channel crosstalks¹. Various schemes have been proposed to realize on-chip interleavers²⁻⁵. To achieve boxlike spectral response, ring-assisted Mach-Zehnder interferometer (MZI) structures were used to improve the sharpness of the interleavers³⁻⁵. However, these schemes exhibit large device footprints since large radii of ring resonators are needed to meet the requirement of narrow channel spacing. In addition, the length difference of the two interfering arms needs to be half of the ring circumference. A silicon photonic interleaver using loop-mirror-based Michelson-Gires-Tournois interferometer was recently proposed and experimentally demonstrated⁶, which takes advantages of reflective optical paths to reduce the footprint, but requires a length difference of the two arms equal to half of the cavity length. A ring-resonator MZI interleaver⁷ consisting of a ring resonator and a directional coupler eliminated the requirement of the length difference of the two arms. However, it still has a large cavity length if narrow channel spacing is needed.

In this paper, we propose and experimentally demonstrate a compact silicon photonic interleaver with boxlike spectral response using an interfering loop containing a Fabry-Perot (FP) cavity formed by two Sagnac loop mirrors (SLMs). The proposed interleaver takes advantages of reflective optical paths to reduce the cavity length and improve the wavelength-tuning efficiency⁸. Moreover, the central wavelength can be changed by tuning only one waveguide connecting the two SLMs, without tuning the length difference of the two arms. The designed device is integrated on a silicon-on-insulator (SOI) platform with a footprint of $106.4 \times 55.1 \mu\text{m}^2$. The free-spectral range (FSR) of the interleaver is $\sim 2.09 \text{ nm}$. The 3-dB and 20-dB bandwidths of the passband are $\sim 1.09 \text{ nm}$ and

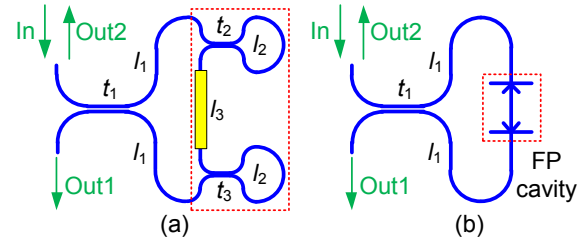


Fig. 1: (a) Schematic of the proposed interleaver. (b) An equivalent structure of the interleaver. FP: Fabry-Perot.

$\sim 1.585 \text{ nm}$, respectively, thus the 20-to-3 dB bandwidth ratio is ~ 1.45 . By thermally tuning the waveguide connecting the two SLMs, the central wavelength of the interleaver can be shifted. In the experiment, the transmission spectrum is red-shifted by $\sim 2.67 \text{ nm}$ with a heating power of $\sim 37.25 \text{ mW}$.

Device structure and operation principle

The schematic of the proposed interleaver is shown in Fig. 1(a), which is an interfering loop containing a FP cavity formed by two SLMs. It is equivalent to the structure shown in Fig. 1(b). The light launched into the input waveguide is split by a directional coupler. After double passing the FP cavity, the lights interfere and output through the directional coupler. $d = 2l_2 + l_3$ is the cavity length of the proposed interleaver. Based on transfer matrix method⁹, the field transmissions of the loop structure can be given as follows:

$$t_{\text{Out1}} = a_1^2((t_1^2 - k_1^2)t_{\text{FP}} + jt_1k_1(r_{\text{FP1}} + r_{\text{FP2}})), \quad (1)$$

$$t_{\text{Out2}} = a_1^2(t_1^2r_{\text{FP1}} - k_1^2r_{\text{FP2}} + 2jt_1k_1t_{\text{FP}}),$$

$$t_{\text{FP}} = t_{s2}t_{s3}a_3/(1-r_{s2}r_{s3}a_3^2),$$

$$r_{\text{FP1}} = 2ja_2(t_2k_2 + a_2^2a_3^2t_3k_3)/(1-r_{s2}r_{s3}a_3^2),$$

$$r_{\text{FP2}} = 2ja_2(t_3k_3 + a_2^2a_3^2t_2k_2)/(1-r_{s2}r_{s3}a_3^2),$$

where t_{FP} and $r_{\text{FP}i}$ ($i = 1, 2$) are the transmission and reflection functions of the Fabry-Perot (FP) cavity formed by the two SLMs, respectively. t_{si} and r_{si} ($i = 2, 3$) are the field transmission and reflection functions of a SLM⁸. t_i and k_i ($t_i^2 + k_i^2 = 1$, $i = 1, 2, 3$) are the transmission and coupling coefficients of the directional couplers,

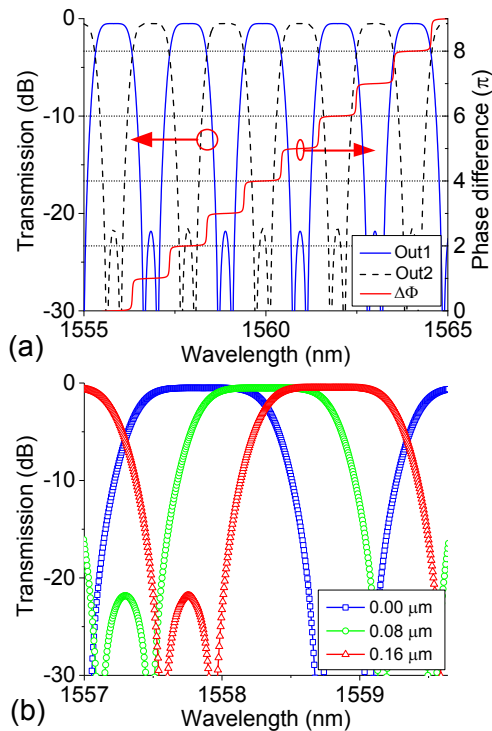


Fig. 2: (a) Transmission spectrum of the interleaver, and the phase difference of the two terms in t_{Out1} . (b) Simulated wavelength tuning of the transmission spectrum.

respectively. $a_i = \exp(-\alpha l_i - j\beta l_i)$ ($i = 1, 2, 3$) are the transmission factors of the waveguides, with l_i ($i = 1, 2, 3$) denoting the lengths of the waveguides. α and $\beta = 2\pi n_G/\lambda$ are the loss factor and propagation constant of the silicon waveguides, respectively, with n_G denoting the group index of the transverse electric (TE) mode. In our simulations, the transmission coefficients t_1 , t_2 , and t_3 are chosen as 0.382, 0.24, and 0.24, respectively. n_G is 4.3525 and α is 10.16 dB/cm. The lengths of the waveguides are $l_1 = 40.89$ μm , $l_2 = 64.83$ μm , and $l_3 = 207.55$ μm , respectively.

Figure 2(a) depicts the simulated transmission spectra of the interleaver. The suppression ratio of the interleaver is higher than 22 dB. The FSR of the spectrum is ~ 2.09 nm. The 3-dB and 20-dB bandwidths of the interleaver are ~ 1.02 nm and ~ 1.54 nm, respectively. Therefore, boxlike passbands with a 20-to-3 dB bandwidth ratio of ~ 1.51 are obtained. The boxlike transmission spectra can be attributed to the interference of the two terms $(t_1^2 - k_1^2)t_{\text{FP}}$ and $j t_1 k_1 (r_{\text{FP1}} + r_{\text{FP2}})$ in the transmission function t_{Out1} . The phase difference $\Delta\Phi$ of the two terms is shown by the red curve in Fig. 2(a), which approaches $2n\pi$ (n is an integer) in the passband, and $(2n+1)\pi$ in the stopband⁶.

The central wavelength of the interleaver can be changed by tuning the phase shifter along l_3 . Since a length difference of the two arms is not needed, the central wavelength tuning is much simplified. The wavelength tuning is simulated

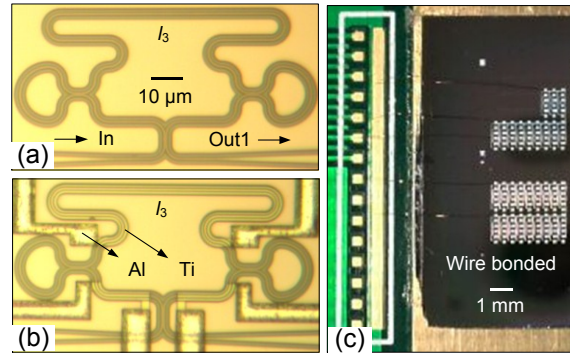


Fig. 3: Micrographs of the chip (a) before and (b) after fabricating Ti heaters and Al pads. (c) The chip on the PCB.

by increasing l_3 to $l_3 + \Delta l_3$. Figure 2(b) presents the transmission spectra of wavelength tuning with Δl_3 changing from 0.00 μm to 0.16 μm . The central wavelength is red-shifted by ~ 0.915 nm.

Device fabrication and measured transmission spectra

The designed device was fabricated on a SOI wafer with a 220-nm-thick top silicon layer and a 3- μm -thick buried oxide layer. E-beam lithography was used to define the device pattern. The top silicon layer was then etched by an inductively coupled plasma (ICP) etching process. The cross-sections of the waveguides are 450×220 nm^2 . A micrograph of the device after etching the top silicon layer is shown in Fig. 3(a). The footprint of the interleaver is 106.4×55.1 μm^2 . A 1- μm -thick silica layer was deposited over the whole device as upper cladding by plasma enhanced chemical vapor deposition (PECVD). 100-nm-thick Ti heaters and 1- μm -thick Al pads were fabricated using lift-off processes, as shown in Fig. 3(b). Fig. 3(c) shows the chip after wire bonding to a printed circuit board (PCB).

A tunable continuous wave (CW) laser was used to scan the fabricated chip with a step size of 5 μm . Grating couplers for TE polarization were used to couple light with single-mode fibers. The measured and fitted transmission spectra at port Out1 of the interleaver are shown in Fig. 4(a). The coupling loss of the fiber coupling system is ~ 13 dB. The insertion loss of the chip is ~ 6 dB. The measured suppression ratio of the interleaver is ~ 22 dB. The ripples in the passband can be attributed to fabrication variation of the directional couplers. The FSR of the spectrum is ~ 2.09 nm, which can be changed by varying l_3 . The measured 3-dB and 20-dB bandwidths are ~ 1.09 nm and ~ 1.585 nm, respectively, which means a 20-to-3 dB bandwidth ratio of ~ 1.45 . The fitting parameters include $t_1 = 0.382$, $t_2 = 0.24$, $t_3 = 0.24$, $n_G = 4.3525$, and $\alpha = 10.16$ dB/cm.

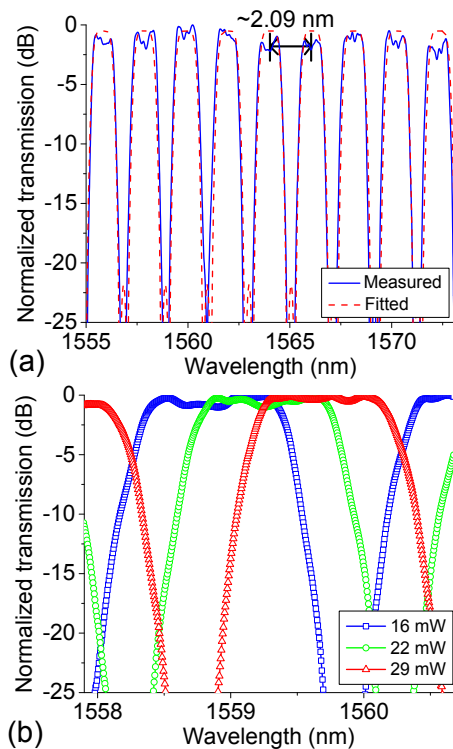


Fig. 4: (a) Measured and fitted transmission spectra. (b) Wavelength tuning by applying different heating powers.

The central wavelength shifting is demonstrated by tuning the heater along I_3 . The central wavelength redshifts as the effective cavity length increases. Figure 4(b) shows the measured transmission spectra of the interleaver by applying different heating powers. The central wavelength was red-shifted by ~ 0.845 nm when the heating power changed from 16 to 29 mW. We also demonstrated wavelength shifts larger than one FSR. The central wavelength increased by ~ 2.67 nm with the heating power changing from 0 to 37.25 mW, corresponding to a wavelength-tuning efficiency of ~ 0.072 nm/mW.

Conclusion

A compact ($106.4 \times 55.1 \mu\text{m}^2$) silicon photonic interleaver with boxlike spectral response using an interfering loop containing a FP cavity formed by two SLMs is proposed and experimentally demonstrated. Compared to ring-based interleavers, the proposed device has a shorter cavity length to achieve the same channel spacing due to the standing-wave characteristic of the FP cavity. Moreover, the central wavelength can be changed by tuning only one waveguide connecting the two SLMs. The FSR of the measured transmission spectrum is ~ 2.09 nm, which can be modified to fit the international telecommunications union (ITU) grids. The 3-dB bandwidth is ~ 1.09 nm and the 20-dB bandwidth is ~ 1.585 nm, thus the 20-to-3 dB bandwidth

ratio is ~ 1.45 . By thermal tuning the device, the central wavelength can be shifted by larger than one FSR with a wavelength-tuning efficiency of ~ 0.072 nm/mW.

Acknowledgements

This work was supported by the 863 High-Tech Program under Grant 2015AA017001. We thank the Center for Advanced Electronic Materials and Devices (AEMD) of Shanghai Jiao Tong University for the support in device fabrication.

References

- [1] S. Cao et al., "Interleaver technology: comparisons and applications requirements," *J. Lightwave Technol.*, Vol. **22**, no. 1, p. 281 (2004).
- [2] T. Mizuno et al., "12.5-GHz spacing compact and low-loss interleaver filter using 1.5% Δ silica-based waveguide," *Photon. Technol. Lett.*, Vol. **16**, no. 11, p. 2484 (2004).
- [3] J. Song et al., "Passive ring-assisted Mach-Zehnder interleaver on silicon-on-insulator," *Opt. Express*, Vol. **16**, no. 12, p. 8359 (2008).
- [4] J. Song et al., "Thermo-optical enhanced silicon wire interleavers," *Photon. Technol. Lett.*, Vol. **20**, no. 24, p. 2165 (2008).
- [5] L. W. Luo et al., "High bandwidth on-chip silicon photonic interleaver," *Opt. Express*, Vol. **18**, no. 22, p. 23079 (2010).
- [6] X. Jiang et al., "Compact silicon photonic interleaver using loop-mirror-based Michelson-Gires-Tournois interferometer," *Proc. OFC, Tu2F.5*, Anaheim (2016).
- [7] J. Song et al., "Proposed silicon wire interleaver structure," *Opt. Express*, Vol. **16**, no. 11, p. 7849 (2008).
- [8] X. Sun et al., "Tunable silicon Fabry-Perot comb filters formed by Sagnac loop mirrors," *Opt. Lett.*, Vol. **38**, no. 4, p. 567 (2013).
- [9] A. Yariv, "Critical coupling and its control in optical waveguide-ring resonator systems," *Photon. Technol. Lett.*, Vol. **14**, no. 4, p. 483 (2002).